Orientational Characteristics of Main-Chain Polymer Liquid Crystals As Revealed by the Rotational Isomeric State Analysis of Deuterium NMR Spectra

Akihiro Abe* and Hidemine Furuya

Department of Polymer Chemistry, Tokyo Institute of Technology, 2-12-1 Ookayama, Meguro-ku, Tokyo 152, Japan. *Received November 2, 1988; Revised Manuscript Received January 9, 1989*

ABSTRACT: Deuterium NMR studies have been performed to elucidate orientational characteristics of ether-type main-chain liquid crystals such as $NCPh_2O(CD_2)_nOPh_2CN$ (DLC I-n; Ph = phenyl) and $[-PhOC(O)PhO(CD_2)_nOPhC(O)OPhO(CH_2)_nO]-_x$ (PLC II-n) with n = 9 and 10. For PLC II-9, some nematic–isotropic biphasic region was transiently observed around T_{NI}. A certain fraction of poorly aligned domains persistently remained in sample PLC II-10 over the nematic temperature range, probably because of the limitation imposed by our NMR apparatus. A RIS analysis of the D NMR spectra is presented. The bond conformation probabilities of the flexible spacer in the nematic phase were estimated for DLC I-n and PLC II-n with n = 9 and 10. The results indicate that the nematic conformation of the flexible segment is amazingly similar between the dimer and polymer with the same n. The difference between these two arises mostly from the orientation of the molecular axis in the liquid-crystalline domain. The orientational order parameters of the mesogenic core axis estimated from these analyses were found to be quite consistent with those observed directly by using mesogen-deuterated samples.

Introduction

In the thermotropic liquid crystals comprising low molecular weight mesogens, anisotropic intermolecular forces play an important role in promoting the parallel alignment of molecules. Mesogens often include *p*-phenylene groups that lie along the molecular axis. In such molecules, the principal axis for the polarizability anisotropy of the phenylene groups also lies in the same direction.[1] The ordering of anisotropic molecules is usually characterized by the orientational order parameter representing the distribution of the long molecular axis around the director of the liquid crystalline domain. The concept of orientation-dependent dispersion interaction introduced by Maier and Saupe[2] was proved to be useful in understanding the molecular ordering of these systems. Recently main-chain polymer liquid crystals (PLC) comprising a rigid mesogenic core and a flexible spacer in a repeating unit have been extensively studied.[3] The simplest example of such spacers may be of the type $-O(CH_2)_nO-$. As easily shown by an examination of a molecular model, a rectilinear alignment of two mesogenic cores separated by a spacer occurs very rarely.[4,5] In fact, accumulation of experimental evidences indicates that the flexible spacer tends to take a highly extended, i.e., trans-rich, conformation in the liquid crystalline state.[4-10] The molecular axis which may be conventionally defined by the tangential vector along the contour of the polymeric chain should not generally coincide with the mesogenic core axis which is closely related to the direction of the polarizability anisotropy. A straightforward application of the Maier–Saupe concept is difficult in these systems.

These PLCs often exhibit a distinct odd–even effect in various thermodynamic quantities at the nematic–isotropic (NI) transition temperature.[3] The orientational order parameter of the mesogenic core axis is also known to oscillate with the number of methylene units n.[11,12] In these systems, the order-disorder transition of the anisotropic mesogenic cores is coupled with conformational changes of the flexible spacer.[3] The conformational rearrangement of the flexible segment taking place at the transition should give rise to a significant contribution to various thermodynamic quantities such as entropy and enthalpy.[4-12] Determination of the conformation permitted in the mesophase is of primary importance in understanding the molecular mechanism of such transitions. The deuterium NMR method has proved to be useful for this purpose.[6-12] The quadrupolar splittings observed in the mesophase provide information regarding the average orientation of the deuterium-labeled bond.

In a previous work,[8] we have developed a model (cf. Figure 1) based on the assumptions that (1) the molecular axis (Z) lies in the direction parallel to the line connecting the centers of two neighboring mesogenic cores, the inclination of the mesogenic core with respect to the Z-axis is denoted by ψ, and (2) the molecules are approximately axially symmetric (at least locally) around the Z-axis, and thus the orientation of these anisotropic molecules can be described by a single order parameter S_{ZZ}. With the molecular axis thus defined, quadrupolar splittings $\Delta\nu_i$ of the ith C–D bond can be expressed by the conventional expression

$$\Delta\nu_i = (3/2)(e^2qQ/h)S_{ZZ}(3\langle\cos^2\phi\rangle - 1)/2 \qquad (1)$$

where e^2qQ/h is the quadrupolar coupling constant, ϕ represents the angle between the C–D bond and the molecular axis, and the brackets denote the statistical mechanical average over all orientations. The conformation of the spacer in the nematic phase can be determined from the observed values of $\Delta\nu_i$. The order parameter S_{ZZ} for the molecular axis and the intramolecular orientational correlation

$$P_2(\cos\psi) = (3\langle\cos^2\psi\rangle - 1)/2 \qquad (2)$$

can also be elucidated concomitantly.[8,13] The order parameter of the mesogenic core axis (S_M) with respect to the director of the domain may be given by the product

$$S_M = S_{ZZ}P_2(\cos\psi) \qquad (3)$$

The validity of the model has been tested for several dimer liquid crystals[8,9] including

$NCPh_2O(CD_2)_nOPh_2CN$
I-n

with n = 9 and 10. In these examples, the values of S_M estimated by eq 3 were found to be consistent with those derived from more direct measurements.

In this work, a similar treatment has been extended to polymer liquid crystals such as

$[-PhOC(O)PhO(CD_2)_nOPhC(O)OPhO(CH_2)_nO]-_x$
II-n

0024-9297/89/2222-2982$01.50/0

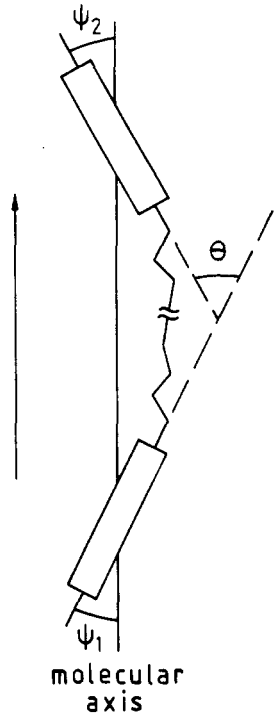

Figure 1. Definition of the molecular axis, angles ψ_1 and ψ_2 representing the inclination of the mesogenic cores.

with n = 9 and 10. As shown above, PLC II comprises two flexible spacers in a repeating unit. Deuterons are introduced only in one kind of spacer in order to enhance the resolution in the D NMR spectroscopy. Some preliminary results were reported previously.[10] Both compounds I and II bear a common structural feature in the spacer. Comparison between the two should lead to a more comprehensive understanding of the role of the spacer. In a separate study, the orientational order parameter of the mesogenic core axis (S_M) has been determined for samples carrying deuterated aromatic cores:

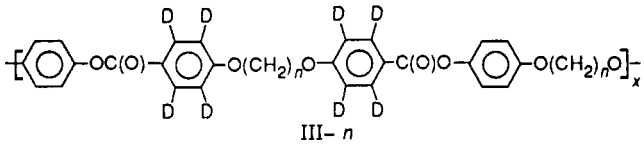

III- n

with n = 9 and 10. Thus, validity of the relation given by eq 3 can be tested for these polymer liquid crystals.

Experimental Section

Samples. Preparation of samples DLC I and PLC II have been described previously.[9,10] Samples PLC III were synthesized by using deuterated 4-hydroxybenzoate. The deuteration reaction was carried out by refluxing a mixture of ethyl 4-hydroxybenzoate and deuterium oxide in the presence of Raney nickel catalyst for 1 week. Deuterium labels were introduced at levels of 10% on the 2,6-positions and 86% on the 3,5-positions of the aromatic ring.

The intrinsic viscosities of PLC II were measured in a mixture of phenol (60%) and 1,1,2,2-tetrachloroethane (40%) at 30 °C:[14] $[\eta]$ = 0.62 and 0.46 dL g^{-1}, respectively, for II-9 and II-10.

All samples exhibited an enantiotropic nematic mesophase by the polarizing microscopic examination. The transition temperatures (°C) determined by DSC are as follows:

DLC I-9: K 134 N 170 I
I-10: K 165 N 184 I

PLC II-9: K 140 N 200 I
II-10: K 169 N 204 I

Measurements. The NMR spectra were recorded on a JEOL JNM-GSX-270 Fourier transform spectrometer operating at 41.3-MHz deuterium resonance frequency. Measurements were carried out under a complete proton decoupling and nonspinning mode. In most experiments, samples initially kept at a temperature above T_{NI} were cooled slowly to turn into the nematic mesophase. Since PLC II-10 has T_{NI} higher than the limit (200 °C) of the JEOL apparatus, the sample was kept at 200 °C for a prolonged time prior to the measurement.

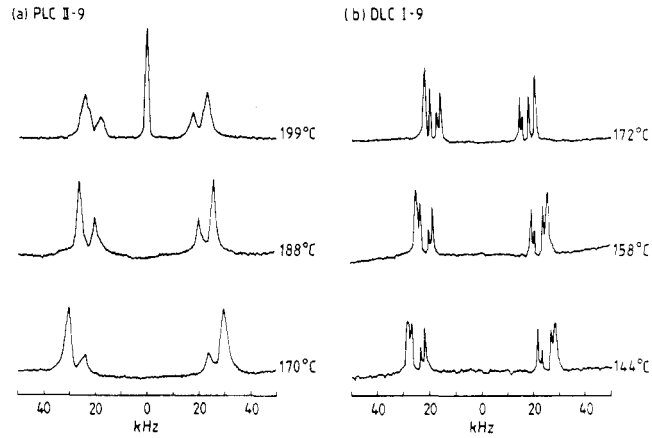

Figure 2. D NMR spectra of samples with n = 9 observed at temperatures as indicated: (a) polymer (II-9) and (b) dimer (I-9).

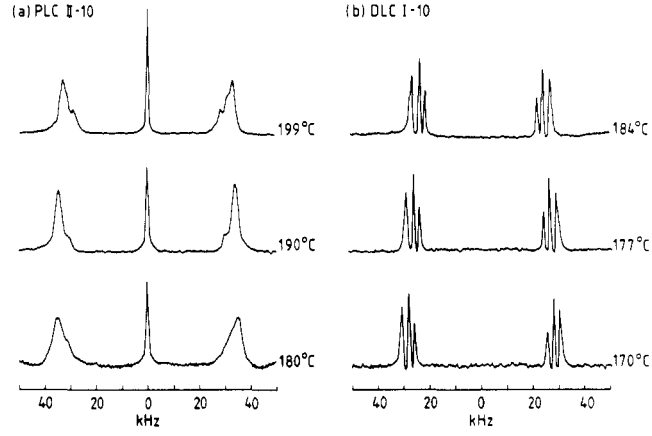

Figure 3. D NMR spectra of samples with n = 10 observed at temperatures as indicated: (a) polymer (II-10) and (b) dimer (I-10).

Deuterium NMR Spectra

Shown in Figures 2 and 3 are the D NMR spectra of samples carrying deuterated spacers. Variations of the profiles in the nematic state were followed by lowering the temperature. In these figures, the spectra obtained for the polymer are compared with those of the dimer having a spacer of the same parity. For PLC II-9 (Figure 2a), some NI biphasic region was transiently observed at around T_{NI}. Since we were obliged to run our measurements below 200 °C (i.e., the upper limit of the JEOL apparatus), samples PLC II-10 never reached their T_{NI} in the NMR magnet. In Figure 3a, a sharp peak was persistently observed at the center of the spectra throughout the nematic temperature range, indicating that some poorly aligned domains remained under the experimental condition. In Figures 2 and 3, the polymers exhibit somewhat larger quadrupolar splittings than the corresponding dimers. The general profiles of the spectra are quite similar between the polymer and dimer with the same n. The dimer samples are less viscous, and therefore the resolution of the signal is better in Figures 2b and 3b. For n = 9, the four splittings observed in Figure 2b (I-9) are transformed into two doublets with broad peaks in Figure 2a (II-9): the peak intensity ratio varies from 4:2:1:2 to 2:1. With n = 10, sample II-10 exhibits a doublet with two shoulder peaks

Table I
Quadrupolar Splittings Observed in the Vicinity of T_{NI}

compd	temp, °C	$\Delta\nu_{obsd}$, kHz	$\Delta\nu_{obsd}/\Delta\nu_1$[a]
PLC II-9	188	52.0	1.0
		40.1	0.77
PLC II-10	199	64.7	1.0
		62.3	0.96
		56.7	0.88
DLC I-9	172	42.0	1.0
		38.0	0.90
		32.1	0.76
		30.4	0.72
DLC I-10	184	53.5	1.0
		47.7	0.89
		43.6	0.81

[a] Ratio of the splittings expressed relative to the largest $\Delta\nu$ value.

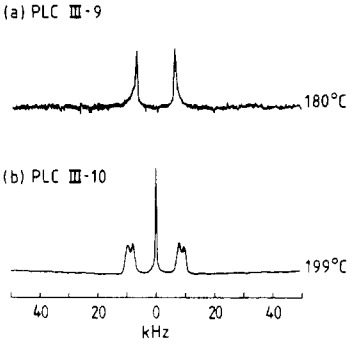

Figure 4. D NMR spectra of PLC samples III-n having partially deuterated mesogenic cores observed at temperatures as indicated: (a) n = 9 and (b) n = 10.

(Figure 3). The fine profile of I-10 (Figure 3b) becomes somewhat obscure in the polymer spectrum (Figure 3a), but the correspondence between the two is still recognizable.

Numerical values of the splittings observed just below T_{NI} are summarized in Table I. The assignment of the individual splittings to the methylene groups of the spacer has been worked out previously by using partially deuterated DLC samples.[9] The results may be summarized as follows:

DLC I-9: $\Delta\nu_1 = \alpha$ and β, $\Delta\nu_2 = \delta$, $\Delta\nu_3 = \epsilon$, $\Delta\nu_4 = \gamma$

DLC I-10: $\Delta\nu_1 = \alpha$ and β, $\Delta\nu_2 = \gamma$ and δ, $\Delta\nu_3 = \epsilon$

Shown in the last column of Table I are the observed ratios expressed relative to the largest splittings $\Delta\nu_1$. The expression given in eq 1 suggests that the ratio between the two $\Delta\nu$ values should be free from the order parameter of the molecular axis S_{ZZ}; thus

$$\Delta\nu_i/\Delta\nu_1 = (3\langle\cos^2\phi_i\rangle - 1)/(3\langle\cos^2\phi_1\rangle - 1) \quad (4)$$

The right-hand side of this expression includes terms such as $\langle\cos^2\phi\rangle$, an average that solely depends on the spatial configuration of the flexible spacer. As shown in a later section, eq 4 provides a basis for the RIS simulation of the D NMR spectra.

Shown in Figure 4 are the D NMR spectra obtained from PLC III carrying partially deuterated mesogenic cores. The spectrum for III-9 (Figure 4a) was obtained at 180 °C. At higher temperatures, a sharp peak appears at the center of the spectrum in addition to the doublet. This sample exhibited an NI biphasic region over a considerably wide temperature range. In the case of III-10 (Figure 4b), the signal located at the center of the spectrum remained over the entire nematic temperature range, essentially the same behavior being observed for sample II-10 (cf. Figure 3a). The spectrum shown in Figure 4b comprises two quadrupolar splittings, indicating that the orientational orders of the deuterons at the 2,6- and 3,5-positions on the aromatic ring are unequal in the nematic field. In sample III-9, such a disparity seems to be practically averaged out in the nematic field (Figure 4a). The order parameters of the mesogenic core axis (S_M) were obtained from these spectra according to the procedure previously adopted in the D NMR studies of some ester DLCs.[11] The deviation from the axial symmetry inherent to the mesogenic core was estimated from the observed $\Delta\nu$ values of III-10.[15] The same correction was adopted in the analysis of the spectrum of III-9. The order parameters S_M thus estimated are 0.45 for III-9 (180 °C, cf. Figure 4a) and 0.69 for III-10 (199 °C, cf. Figure 4b). For III-9, a somewhat lower value, S_M = 0.39, was obtained from the data derived at 190 °C.

RIS Analysis

Geometrical Data. Bond lengths and bond angles required for the RIS description of the flexible spacer were taken from Table II of the previous paper.[8] Following the previous treatment, the mesogenic cores are treated as a simple rod with a center at a distance of 5 Å from the oxygen atom, the value roughly corresponding to the structures illustrated in the introductory part. The methylene carbons of the flexible spacer are numbered from one terminal to the midchain:

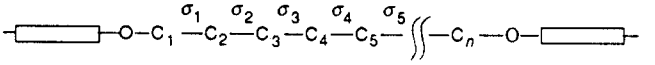

Because of the symmetry of the molecules, distinction beyond the middle is redundant. Statistical weight factor σ_i was assigned to the gauche state of the ith C–C bond, the weight of unity being given to the corresponding trans state.

Conformational Distribution on the (ψ_1,ψ_2) Map. The RIS calculations were first performed for molecules in the unconstrained isotropic state, thereby all possible conformations of the spacer, $-O(CH_2)_nO-$, being elucidated.[4,5,16] Conventional values of the conformational energy parameters were adopted in these calculations: $E_{\sigma_1} = 0$, $E_{\sigma_i} = 0.5$ with i = 2–5, $E_\omega = 2.0$ for the second-order interaction involved in

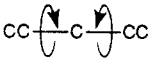

and $E_{\omega'} = 0.5$ for

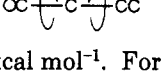

all energies being in kcal mol^{-1}. For simplicity, the temperature was set equal to 500 K. For each conformation of the spacer, the inclination angles ψ_1 and ψ_2 (see Figure 1) were calculated. The distributions of the conformation (ψ_1,ψ_2) thus estimated are indicated on the map as shown in Figure 5, where the population densities of the conformation (per 5°×5° square) are distinguished into three ranks: heavily dotted (>1.0%), moderately dotted (0.1–1.0%), and lightly dotted area (<0.1%). As required by the chemical structure of the molecule, diagrams 5a and 5b are symmetric around $\psi_1 = \psi_2$, respectively, for both n = 9 and 10. The distributions are bimodal, being consistent with the results of the previous RIS analysis where distributions were studied as a function of the angle θ between the two successive mesogenic core axis (cf. Figure 1).[4,5] It was pointed out in the previous treatment that when the spacer was jointed with the mesogenic cores by the ether or ester linkages, the distribution curves $f(\theta)$ – θ exhibited very distinct odd–even characteristics with the

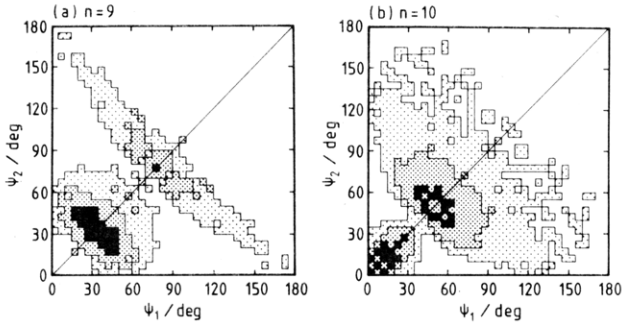

Figure 5. Conformational distribution map (ψ_1,ψ_2) calculated for a sequence such as $-MO(CH_2)_nOM-$ (M: mesogenic core) in the unconstrained isotropic state: (a) $n = 9$ and (b) $n = 10$. The population densities of the conformation (per 5°×5° square) are distinguished into three ranks: heavily dotted (>1.0%), moderately dotted (0.1–1.0%), and lightly dotted (<0.1%).

number of methylene units of the spacer. For the ether-type PLC with $n = 9$, the major portion of the angle θ is located in the range 50–80° (84%), and to some extent (16%) in the region above 150°. When $n = 10$, the angle is distributed in the range 0–20° (32%) and 90–120° (68%). The (ψ_1,ψ_2) maps shown in Figure 5 afford a clear understanding of the molecular mechanism involved in the transition from the isotropic to the nematic state. The uniaxial arrangement of the neighboring mesogenic cores may be most closely satisfied in the system with n = even, where a significant fraction of $\psi_1,\psi_2 < 30°$ (Figure 5b) is found. In contrast, the inclination angle ψ exceeds 30° in most of the conformers with n = odd (Figure 5a).

Elucidation of the Nematic Conformation by the Simulation of the Deuterium NMR Spectra. Under a nematic environment, distribution of the conformer should be restricted within certain ranges of the (ψ_1,ψ_2) map. To save computer time, configurations that do not conform to the nematic ordering were discarded: for n = 9, $\psi_1,\psi_2 > 45°$ and for $n = 10$, $\psi_1,\psi_2 > 40°$. Thus, conformations in the colony with larger ψ values were dismissed. For the nematic conformation, the second-order interactions $g^{\pm}g^{\mp}$ were assumed to be entirely suppressed. For all of the spatial configurations thus selected, the orientation of the constituent C–D bonds was calculated in terms of $\cos^2\phi$. The average $\langle\cos^2\phi\rangle$ for a given C–D bond may be expressed as

$$\langle\cos^2\phi\rangle = \sum_k[\cos^2\phi(\prod_{i=1}^{n-1}s_i)]_k/\sum_k(\prod_{i=1}^{n-1}s_i)_k \qquad (5)$$

where s_i represents the weight for bond i, i.e., 1 or σ_i, in the kth configuration. In the simulation, statistical weight parameters σ_i (i = 1 to n − 1) were varied in an uncorrelated manner within the range 0–1. Use of eq 4 may yield $\Delta\nu_i$ with either a positive or negative sign. Comparison with experimental observations requires only absolute values of $\Delta\nu_i$. Computations were iteratively repeated until the calculated value of $|\Delta\nu_i/\Delta\nu_1|$ reproduced the observed profile of the D NMR spectrum. A unique set of statistical weight factors was successfully selected for each molecular system by this technique.

The simulations were first carried out for the dimer. The statistical weight parameter set thus derived was adopted as the initial set in the simulation of the corresponding polymer spectrum.

Results and Discussion

Examples of the RIS simulation are illustrated in Figure 6, where the observed spectra are compared with the stick diagrams derived from the calculation: the results for n = 9 are illustrated in diagrams 6a and 6b, and those for

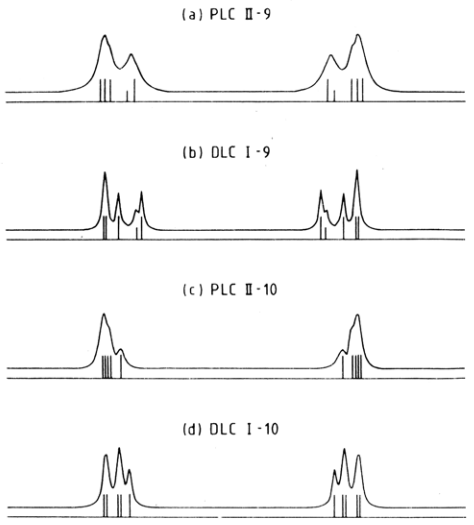

Figure 6. Comparison of the results of the RIS simulation (stick diagrams) with the observed D NMR profiles: (a) PLC II-9, (b) DLC I-9, (c) PLC II-10, and (d) DLC I-10.

Table II
Bond Conformations of the Flexible Spacer Estimated from the Deuterium NMR Data Given in Table I[a]

	PLC		DLC	
bond	II-9	II-10	I-9	I-10
C_1–C_2	0.57 (0.36)	0.36 (0.36)	0.54 (0.36)	0.42 (0.36)
C_2–C_3	0.77 (0.55)	0.97 (0.55)	0.74 (0.57)	0.92 (0.56)
C_3–C_4	0.51 (0.58)	0.48 (0.58)	0.50 (0.59)	0.50 (0.59)
C_4–C_5	0.67 (0.58)	0.91 (0.58)	0.64 (0.59)	0.86 (0.58)
C_5–C_6		0.48 (0.58)		0.50 (0.58)

[a] Values in parentheses are those calculated for the isotropic state.

$n = 10$ in 6c and 6d. Corresponding to the expression given in eq 4, the peak separations are normalized against the largest splitting $\Delta\nu_1$ in each diagram. As in the simulation, the positional order of the peaks was observed to be identical between the polymer and the dimer. From the values of σ_i estimated above, bond conformations expressed in terms of the trans fraction, $f_t = 1 - f_g$, can be easily evaluated. The results are summarized in Table II, where for comparison, values of f_t calculated for the isotropic state at the same temperature are also included in parentheses: the conformational energy parameters required in the latter calculations were given in the preceding section. As shown in the table, the difference between the polymer and dimer is rather small for both n = 9 and 10, indicating that the conformation permitted in the nematic phase is similar. The odd–even alternation of the f_t value along the chain is very marked for $n = 10$. Such a trend becomes less distinct for n = 9. For the dimer and polymer of $n = 10$, the profiles of the D NMR spectrum vary rather insensitively with the conformation around the bonds such as C_3–C_4 and C_5–C_6. As pointed out by Yoon et al.,[7] these bonds tend to align parallel with the mesogenic core axis in the nematic conformation. In the above treatment, conformational statistical weights of these bonds were somewhat arbitrarily set equal to the values usually adopted in the isotropic state.

Various characteristics of the nematic phase at the NI transition were estimated and are listed in Table III. In these calculations, the energy difference between the gauche and trans state was taken to be intrinsically invariant for a given bond in both the nematic and isotropic phase. The nematic fractions thus estimated are of the order of 10% in both the dimer and polymer liquid crystals. The conformational contribution to the entropy

Table III
Characteristic Properties of the Nematic Phase Estimated from the Deuterium NMR Data Given in Table I

	PLC		DLC	
	II-9	II-10	I-9	I-10
f_N/%	8.85	10.49	14.84	9.35
$\Delta\langle E\rangle_{NI,conf}$/(kcal mol^{-1})	0.50	0.88	0.36	0.77
$\Delta S_{NI,conf}$/(cal mol^{-1} K^{-1})	5.88	6.33	4.60	6.40
$P_2(\cos\psi)$	0.55	0.93	0.55	0.92
S_{ZZ}	0.71	0.69	0.58	0.57
S_M				
$S_{ZZ}P_2(\cos\psi)$	0.39	0.64	0.32	0.52
obsd	0.39[a]	0.69,[a] 0.75[b]	0.33[c]	0.50[c]

[a] This work. [b] Reference 7. [c] Reference 12.

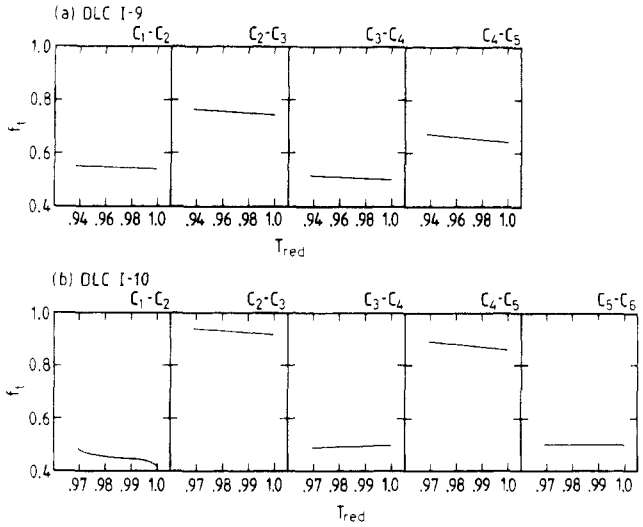

Figure 7. Bond conformation probabilities estimated for DLCs. The f_t values are plotted as a function of the reduced temperature $T_{red} = T/T_{NI}$, the temperature being expressed in kelvin: (a) DLC I-9 and (b) DLC I-10. The bond orders are indicated on each diagram.

change ΔS_{NI} exceeds those directly observed for the corresponding samples. While the intramolecular orientational correlation term, $P_2(\cos\psi)$, exhibits a large odd–even oscillation with n, the orientational ordering of the molecular axis S_{ZZ} with respect to the nematic director is nearly of the same order for both $n = 9$ and 10. For a given n, the variation of $P_2(\cos\psi)$ from the dimer to the polymer is very small. In contrast, the value of S_{ZZ} tends to be enhanced in the polymeric system. As defined by eq 3, the product of these two order parameters should give rise to the orientational order parameter of the mesogenic core axis. The values of S_M thus estimated are given in the sixth row of Table III. The corresponding values of S_M determined directly by using mesogen-deuterated samples are listed in the last row, where experimental values reported in the literature are also included. The agreement between the S_M values estimated by the direct and indirect methods are excellent for all PLCs and DLCs examined. These results suggest that the odd–even characteristics observed in S_M arise mainly from the $P_2(\cos\psi)$ term. Thus, present analysis provides a reasonable molecular scheme that is consistent with experimental observations derived from both the flexible spacer and the mesogenic core.

The quadrupolar splittings observed at different temperatures may be treated in a similar manner. Bond conformation probabilities were elucidated for DLCs for which the D NMR spectra were obtained in high resolution over a wide temperature range. In Figure 7, variations of the bond conformation are plotted separately for the individual bonds as a function of the reduced temperature $T_{red} = T/T_{NI}$, temperatures being expressed in kelvin. For most of the bonds, the f_t values tend to increase slightly

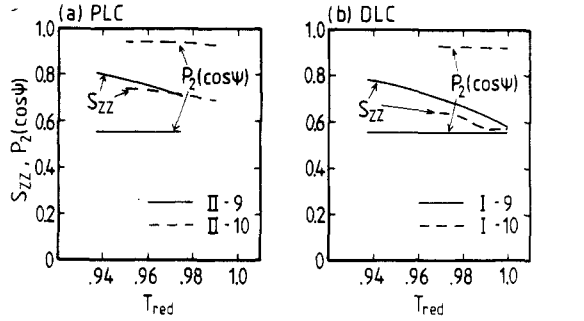

Figure 8. Variations of the order parameter S_{ZZ} and the intramolecular orientational correlation $P_2(\cos\psi)$ with the reduced temperature: (a) PLCs II-9 (solid) and II-10 (dotted); (b) DLCs I-9 (solid) and I-10 (dotted).

as the temperature decreases. For the reason stated above, values of f_t for C_3–C_4 and C_5–C_6 of DLC I-10 remain nearly invariant with temperature. An analogous trend was found for the corresponding polymers, although the f_t values obtained are somewhat less accurate because of the poor resolution of the polymer spectra. These results indicate that the nematic conformation of the spacer may not be much affected by the temperature.

Shown in Figure 8 is the temperature dependence of the order parameters such as $P_2(\cos\psi)$ and S_{ZZ}. For a given n, the difference between the polymer (Figure 8a) and dimer (Figure 8b) is amazingly small. In all the systems examined, the values of $P_2(\cos\psi)$ remain nearly constant with temperature, while those of S_{ZZ} increase substantially with decreasing temperature.

Concluding Remarks

The DLCs and PLCs investigated in this work bear an identical flexible spacer $-O(CH_2)_nO-$, but they differ somewhat in the chemical structure of the mesogenic cores. In the aforementioned analysis, mesogens are treated as a simple rod 10 Å long. In PLC II, however, the distance spanning the two ether oxygens located on both sides of the mesogenic core amounts to ca. 12 Å. For comparison, the analysis of the D NMR data was also carried out by adopting mesogenic cores of this length. The effect proved to be practically nil for PLC II-10. For PLC II-9, the f_t values around C_1–C_2 and C_3–C_4 were slightly enhanced: an increment of 0.03 and 0.05, respectively, relative to those listed in Table II. Accordingly, the nematic fraction f_N increases by 0.4% (cf. Table III). The physical properties estimated for this fraction were found to be nearly identical with those of the previous calculation.

An important consequence of the present analysis is that the nematic conformation of the flexible segment is very similar between the dimer and polymer of a given n. The difference arises in the orientation of the molecular axis in the liquid-crystalline domain. The order parameter S_{ZZ} becomes higher in the polymeric system.

The spacer is allowed to take various conformations in as much as they are compatible with the preferred orientation of the mesogenic cores. Under these circumstances, the spacer is fairly extended, and thus participates in the anisotropic intermolecular interactions in the nematic field. It may also be important to note that the f_t values estimated for the individual bonds of the spacer remain quite insensitive to the variation of temperature. In this respect, the flexible spacer maintains liquidlike characteristics in the nematic state.

The molecular scheme described above requires an extension of the polymeric chain with a large persistence length, unless some folds or defects are occasionally involved. Above the NI transition temperature, the conformational restriction imposed by the nematic field should vanish. In the isotropic state, the random-coil conforma-

tion becomes most stable.[16] Then, a question arises regarding how sharp is the transition from a highly extended form to a coil. The D NMR method is sensitive only to short-range correlations. To answer the question, a combined use of some other technique such as the small-angle neutron diffraction[17] is needed.

Acknowledgment. This work was supported in part by a grant-in-aid for Scientific Research on Priority Areas, New Functionality Materials-Design, Preparation and Control, The Ministry of Education, Scientific and Culture (63604531).

Registry No. I-*n* (*n* = 9), 119908-59-7; I-*n* (*n* = 10), 119908-60-0; II-*n* (*n* = 9, SRU), 119908-61-1; II-*n* (*n* = 10, SRU), 119908-62-2; II-*n* (*n* = 9, copolymer), 119080-27-2; II-*n* (*n* = 10, copolymer), 119080-29-4.

References and Notes

(1) Flory, P. J. *Adv. Polym. Sci.* **1984**, *59*, 1. Irvine, P. A.; Flory, P. J. *J. Chem. Soc., Faraday Trans. 1* **1984**, *80*, 1821.
(2) Maier, W.; Saupe, A. *Z. Naturforsch.* **1959**, *14A*, 882; **1960**, *15A*, 287.
(3) *Polymer Liquid Crystals*; Ciferri, A., Krigbaum, W. R., Meyer, R. B., Eds.; Academic: New York, 1982. *Polymeric Liquid Crystals*; Blumstein, A., Ed.; Plenum: New York, 1983. *Recent Advances in Liquid Crystalline Polymers*; Chapoy, L. L., Ed.; Elsevier: London, 1985. Vertogen, G.; de Jeu, W. H. *Thermotropic Liquid Crystals, Fundamentals*; Springer-Verlag: Berlin, 1987.
(4) Abe, A. *Macromolecules* **1984**, *17*, 2280.
(5) Abe, A.; Furuya, H. *Kobunsi Ronbunshu* **1986**, *43*, 247.
(6) Samulski, E. T.; Gauthier, M. M.; Blumstein, R. B.; Blumstein, A. *Macromolecules* **1984**, *17*, 479. Griffin, A. C.; Samulski, E. T. *J. Am. Chem. Soc.* **1985**, *107*, 2975. Samulski, E. T. *Faraday Discuss. Chem. Soc.* **1985**, *79*, 7.
(7) Yoon, D. Y.; Bruckner, S. *Macromolecules* **1985**, *18*, 651. Yoon, D. Y.; Bruckner, S.; Volksen, W.; Scott, J. C.; Griffin, A. C. *Faraday Discuss. Chem. Soc.* **1985**, *79*, 41. Bruckner, S.; Scott, J. C.; Yoon, D. Y.; Griffin, A. C. *Macromolecules* **1985**, *18*, 2709.
(8) Abe, A.; Furuya, H.; Yoon, D. Y. *Mol. Cryst. Liq. Cryst.* **1988**, *159*, 151.
(9) Abe, A.; Furuya, H. *Polym. Bull.* **1988**, *19*, 403.
(10) Furuya, H.; Abe, A. *Polym. Bull.* **1988**, *20*, 467.
(11) Toriumi, H.; Furuya, H.; Abe, A. *Polym. J.* **1985**, *17*, 895.
(12) Emsley, J. W.; Luckerhurst, G. R.; Shilstone, G. N. *Mol. Phys.* **1984**, *53*, 1023. Emsley, J. W.; Heaton, N. J.; Luckerhurst, G. R.; Shilstone, G. N. *Mol. Phys.* **1988**, *64*, 377.
(13) Abe, A.; Furuya, H. *Mol. Cryst. Liq. Cryst.* **1988**, *159*, 99.
(14) Griffin, A. C.; Havens, S. J. *J. Polym. Sci., Polym. Phys. Ed.* **1981**, *19*, 951.
(15) In this treatment, the asymmetric parameter η was taken to be 0.06. From the geometry previously adopted,[11] the principal components of the ordering matrix S_{ZZ}, $S_{XX} - S_{YY}$ were estimated. For notations, see the reference cited: *Nuclear Magnetic Resonance of Liquid Crystals*; Emsley, J. W., Ed.; Reidel: Dordrecht, 1985; pp 379.
(16) Flory, P. J. *Statistical Mechanics of Chain Molecules*; Weley: New York, 1969.
(17) Cotton, J. P.; Decker, D.; Benoit, H.; Farnoux, B.; Higgins, J.; Jannink, G.; des Cloizeaux, J.; Ober, R.; Picot, C. *Macromolecules* **1974**, *7*, 863. Hayashi, H.; Flory, P. J.; Wignall, G. D. *Macromolecules* **1983**, *16*, 1328. Hayashi, H.; Flory, P. J. *Physica* **1983**, *120B*, 408.

Addition of Difluorocarbene to Poly(1,1-dimethyl-1-sila-*cis*-pent-3-ene) and Poly(1,1-dimethyl-1-sila-*cis*-(and -*trans*)-pent-3-ene). Characterization of Microstructures by ^{1}H, ^{13}C, ^{19}F, and ^{29}Si NMR Spectroscopies

Qingshan Zhou and William P. Weber*

K. B. and D. P. Loker Hydrocarbon Research Institute, Department of Chemistry, University of Southern California, Los Angeles, California 90089-1661.
Received August 29, 1988

ABSTRACT: Difluorocarbene, generated by the sodium iodide catalyzed decomposition of (trifluoromethyl)phenylmercury, adds stereospecifically to the carbon–carbon double bonds of poly(1,1-dimethyl-1-sila-*cis*-pent-3-ene) (I) as well as to those of poly(1,1-dimethyl-1-sila-*cis*-(and -*trans*)-pent-3-ene) (II) to yield product polymers of increased molecular weight. The microstructures of these difluorocarbene adduct polymers were characterized by ^{1}H, ^{13}C, ^{19}F, and ^{29}Si NMR spectroscopy. Their thermal stabilities were determined by thermogravimetric analysis. They were considerably less stable than the starting polymers I or II. Their molecular weight distributions were determined by gel permeation chromatography.

There is considerable interest in the chemical modification of polymers.[1-4] Dichloro-[5-8] and difluorocarbene[9] have been added stereospecifically to the carbon–carbon double bonds of *cis*- and *trans*-1,4-polybutadiene.

We were interested in the stability of the polymers formed by the addition of difluorocarbene to the carbon–carbon double bonds of poly(1,1-dimethyl-1-sila-*cis*-pent-3-ene) (I)[10] and to those of poly(1,1-dimethyl-1-sila-*cis*-(and *trans*)-pent-3-ene) (II),[11] since we have previously found that polymers formed by addition of dichlorocarbene to I and II undergo facile chain scission at low temperature (25 °C).[11] This degradation process probably occurs by a two-step mechanism. The first involves ionization of one of the carbon–chlorine bonds with concerted disrotatory opening of the cyclopropane ring to yield a silyl-stabilized allylic cation. It is well-known that silicon has a profound stabilizing effect on β-carbocation centers.[12] This is followed by nucleophilic attack by the chloride anion on an adjacent dimethylsilyl center which results in scission of the polymer chain (see eq 1).

The difluorocarbene adduct polymers of I and II would be expected to be more stable than the corresponding dichlorocarbene adduct polymers, if the first step in this process were rate determining since ionization of a carbon–fluorine bond will occur less readily than that of a carbon–chlorine bond.[13] On the other hand, if nucleophilic attack on the dimethylsilyl center that is β to the allylic carbocation is rate limiting, then we might anticipate that the difluorocarbene adduct polymers would decompose more rapidly since a silicon–fluorine bond is much stronger than a silicon–chlorine bond.[14]

In addition, the difluorocarbene adducts of I and II are most interesting polymers in that their microstructures can be analyzed by ^{1}H, ^{13}C, ^{19}F, and ^{29}Si NMR spectroscopies.

0024-9297/89/2222-2987$01.50/0